ELSEVIER

Chemical Engineering Journal 134 (2007) 145–152

Chemical Engineering Journal

www.elsevier.com/locate/cej

Syngas formation from gasoline in adiabatic reactor: Thermodynamic approach and experimental observations

L. Bobrova [a,b,*], V. Korotkich [a], V. Sadykov [a,b], V. Parmon [a,b]

[a] *Boreskov Institute of Catalysis, 5, Pr. Ak. Lavrentieva, Novosibirsk 630090, Russia*
[b] *Novosibirsk State University, 2, Pirogova Street, Novosibirsk 630090, Russia*

Abstract

To make viable the large-scale use, generation of hydrogen locally from the petroleum-derived fuels such as gasoline is an attractive way because of the existing production, distribution, and retailing infrastructure. The present work is centered on the syngas formation from gasoline. The thermodynamic equilibrium restrictions on the gasoline reforming process in comparison with isooctane and methane are discussed on the basis of multi-component calculations. To perform the thermodynamic modelling, the real fuel containing 191 hydrocarbon species was specified as an equilibrium distribution of 29 close-cut fractions C3–C10 with well-defined properties. The thermodynamic predictions are in a good correlation with the experimental data obtained in a nearly adiabatic monolith reactor.

Keywords: Gasoline; Syngas formation; Thermodynamic equilibrium restriction; Monolith reactor

1. Introduction

Hydrogen is projected to be one of the primary energy sources in the 21st century. Its combustion and oxidation is pollution free and supplies sufficient energy for transportation and other applications. Hydrogen as a fuel for automotive engines is generally assumed to be coupled with a fuel cell that converts the energy of the fuel into electrical energy without combustion. Hydrogen fuelling of internal combustion engines is of great interest as well. Since today there is no existing extensive hydrogen infrastructure and no commercially viable hydrogen storage technology, conversion of hydrocarbons locally to hydrogen-rich gas is considered a critical intermediate step in the drive to make viable the large-scale use of hydrogen as a fuel for transportation and industrial use and for use in fuel cells [1–4]. The lower efficiency of gasoline as a primary fuel in comparison with e.g. methanol can be compensated by the much higher energy density and larger molar content of hydrogen compared to methanol [5,6]. Generally, the primary fuel is converted first into a hydrogen-rich product gas using air and (or) steam on a catalyst at high temperatures using one of three major techniques: steam reforming, partial oxidation and autothermal reforming. When discussing the three principal pathways, Ahmed and Krumpelt [7] demonstrate that the partial oxidation and autothermal reforming processes are more attractive for practical applications; contrary to widely held beliefs, they are also capable of higher reforming efficiencies than are steam reformers. In practice, the efficiency will depend on the specific system design, heat transfer looses, kinetic limitations, and energy required by other components in balance-of-plant.

The development of an efficient reformer for the production of hydrogen from liquid hydrocarbon fuels such as gasoline is very challenging. It requires the development of a stable catalyst for the process. It also requires detailed thermodynamic and kinetic information about the reaction. However, gasoline fuel is a variety of different hydrocarbons. To discover thermodynamic restrictions on the gasoline reforming processes, more simple model fuels consisting of a mixture of hydrocarbons are preferred [8–10]. It is known that at full conversion of hydrocarbons, irrespective of whether a thermal or catalytic burner or fixed or fluidized catalyst bed is used, the composition of the product exit gas will be determined by thermodynamic equilibrium at the exit temperature which is determined by the feed composition and reaction heat evolved (adiabatic temperature rise). Obviously, this is only the case if all necessary reactions can take place because the proper catalyst is used, and the residence times in the catalyst bed are long enough [11]. To provide a guidance related to the operating conditions, the thermodynamic

---

[*] Corresponding author at: Boreskov Institute of Catalysis, 5, Pr. Ak. Lavrentieva, Novosibirsk 630090, Russia.

E-mail address: lbobrova@catalysis.ru (L. Bobrova).

1385-8947/$ – see front matter © 2007 Elsevier B.V. All rights reserved.
doi:10.1016/j.cej.2007.03.067

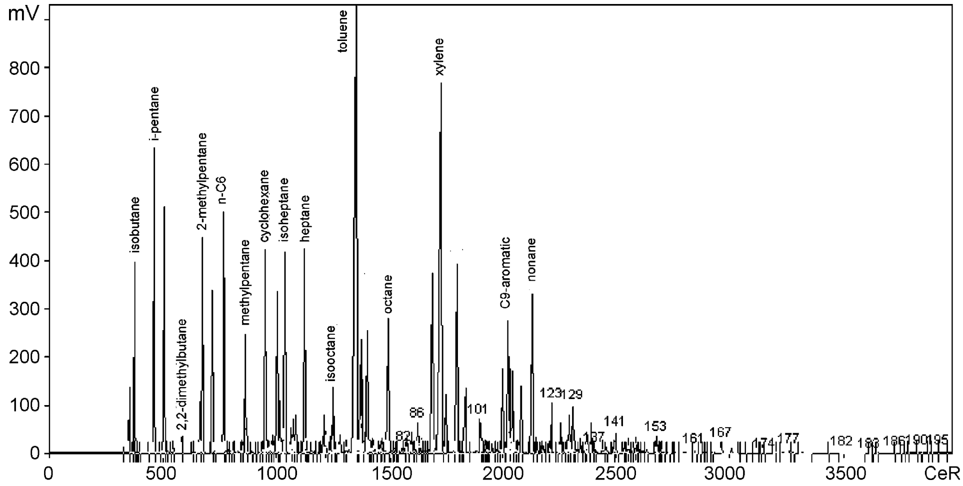

Fig. 1. Chromatogram of reformulated gasoline used in the experiments. The chromatograph HP-5880 operation conditions: DB-1 column 60 m, temperature programming 20–300 °C, 4 °C/min.

equilibrium calculations are useful indeed. Nowadays, thermodynamic theory is even considered to enable the derivation of mass-action kinetics [12,13]. In any case, a correct representation of the thermophysical properties of hydrocarbon fuel is very important to be used in simulations of the fuel processing operations. These can exhibit reasonably similar or distinctly different behavior depending on the composition of the mixture, an effect particularly noticeable with the addition of other reagents. Thus, a model fuel for gasoline is required which is sufficiently flexible to incorporate a large number of compounds/interactions and provide good results [14].

In our previous papers [15,16], the particulars of syngas formation from liquid hydrocarbons such as isooctane and gasoline over LaNiPt/LaRu catalyst washcoated on microchannel ceramics and metallic monoliths were highlighted. Also discussed were few problems encountered with a short contact time reactor operating at a pilot scale, issues that are largely independent of the catalysts employed. Both the product gas composition and temperature at the outlet of the catalytic monoliths were in good agreement with the thermodynamically predicted data. Simulations of syngas formation have been previously performed using isooctane, as a standard reference fuel for gasoline [15]. However, reactivity of different gasoline components was found to affect considerably both the operational parameters and product composition in the reforming process. In the present work, the simulations of gasoline reforming employ a model fuel specified as an equilibrium distribution of 29 close-cut fractions C3–C10 hydrocarbons with the well-defined properties. Experimental observations in a nearly adiabatic monolith reactor with the real gasoline containing 191 hydrocarbon species were accompanied with the thermodynamic calculations by using the model fuel proposed. Some peculiarities about the gasoline reforming process are discussed on the basis of the multi-component calculations in comparison with those for isooctane and methane.

2. Experimental method

The fuel used in the experiments was commercial desulfurized reformulated gasoline. Its composition is illustrated by chromatogram shown in Fig. 1. The 191 types of different hydrocarbons were identified. Amount of aromatics was about 40 wt.%. According to the analysis, the averaged composition of gasoline required to estimate a stoichiometric air/fuel ratio in the feed corresponds to $C_{7.2}H_{13.36}$.

The experiments were carried out in a tubular quartz reactor, approximately 300 mm long and 60 mm inner diameter. The quartz tube was surrounded by an insulation material and immersed into a vertically installed stainless steel reactor of a bigger size. A detailed sketch of the reactor setup has been provided in Ref. [16]. Two identically prepared metallic monoliths each with dimensions of 45 mm long and 55 mm diameter with the span area of 22.96 cm^2 (91.845 cm^3 labour volume) were placed inside. The catalyst support structure (4700 m^2/m^3 specific surface, a void fraction of approximately 80%) was prepared by stacking the flat and corrugated fecraloy foils (50–100 μm thickness) followed by winding them into an Arkhimed spiral (see Fig. 2). A thin (∼5–10 μm) protective corundum sublayer was made up by means of a blast dusting technique [17]. The secondary Ce–Zr–La–O mixed oxide layer (∼10 wt.%) was washcoated by using a standard procedure with alumina hydroxide as a binder. Platinum and $LaNiO_3$ were the basic active components for the next coat. The inlet section of the monolith (about 15 mm) was additionally promoted by Ru + La. Both LaNiPt (1 wt.%) and LaRu (1 wt.%) active compounds were supported via wet impregnation followed by drying and calcinations in air at 900 °C [15,18]. Unloaded monoliths, the 10 mm long fragments of an extruded corundum monolith with a rectangular cross-section (1.9 mm hydraulic diameter) of its channels, were placed in front of and behind the two metallic catalysts to reduce radiation heat loss. Chromel–alumel thermocouples were used to monitor the temperature at various positions along the reactor length, as shown in Fig. 3. The entire reactor ran autothermally at atmospheric pressure. The product composition was determined by gas chromatography (TCD, FID) [16]. A fraction of product gas was taken directly immediately beyond the monoliths package. The fuel feed was delivered to the reactor through a stainless steel tube of 28 mm ID and 1.5 m height filled with inert porcelain rings. The tube

Fig. 2. A view of metallic catalyst supports used in the experiments.

was placed inside a fluidized bed heater-thermostat to ensure uniform temperature profile along the tube. The total flow rate of gasoline, air, and steam to the reactor was varied between 3.5 and 11 m^3/h (STD). The feed stoichiometry is given as the oxygen-to-carbon ratio (O_2/C), which is defined as the moles of dioxygen divided by the moles of carbon in the feed, and water-to-carbon ratio (H_2O/C), which is defined as the moles of water divided by the moles of carbon in the feed.

To ignite the reaction, the feed flow consisted of 1.86 kg/h gasoline, 7.09 m^3/h air (STD), and 1.3 kg/h water ($O_2/C = 0.49$, $H_2O/C = 0.48$) was fed at 270 °C into preheated (by air at 300 °C) reactor. That enabled to avoid a sharp increase of the surface temperature in the frontal part of the catalytic bed during ignition. The flow rate of 9.12 m^3/h results in a flow velocity of 1 m/s with a contact time of approximately 0.07 s (calculating at STD). After ignition the flow rates and compositions of the inlet reactants (including distilled water addition) were altered according to a working plan. One can see in Fig. 3 that doubling the flow rate at the constant oxygen-to-carbon ratio slightly affects the temperature distributions in the reactor. Based on this fact the experimental data obtained at different flow rates but at the constant oxygen-to-carbon ratio were combined at the data processing.

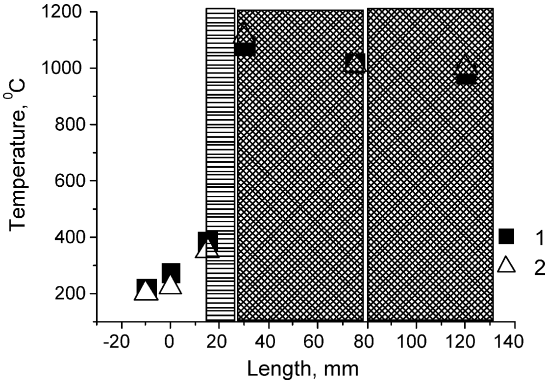

Fig. 3. The temperature profiles along the reactor axis at the steady state: (1) the feed: 0.893 kg/h gasoline, 3.31 m^3/h air (STD) ($O_2/C = 0.48$), $U_0 = 0.42$ m/s and 0.19 s contact time, $T_{in} = 220$ °C; (2) the feed: 1.86 kg/h gasoline, 6.90 m^3/h ($O_2/C = 0.48$), $U_0 = 0.9$ m/s and 0.09 s contact time, $T_{in} = 206$ °C.

By using commercial gasoline as a fuel, we have studied the effect of the feed composition on the outlet temperature and product gas. The experimental data are compared with the results of accompanying thermodynamic modelling, the latter achieved by using a surrogate mixture proposed.

3. Thermodynamic approach

Calculating the composition in a carbon/hydrogen/dioxygen system at chemical equilibrium can be done by either specification of possible reactions taking place or minimizing the total Gibbs free energy in the given chemical system. The equilibrium describes the temperature of the system and the product composition. This requires identification of the possible components, for which thermochemical data must be available. Gasoline fuel is a mixture of normal paraffins, isoparaffins, cycloalkanes, aromatics and olefins. For the simulation, gasoline was represented as a surrogate mixture of the equilibrated close-cut fractions C3–C10 (Table 1) that had a similar carbon-

Table 1
Model fuel mixture exhibiting similar characteristics to gasoline

N	Component	C	H	Mass fraction (w/w, %)	$\Delta_f H°$ (kcal/mol)
1	Isobutane	4	10	0.430	−37.87
2	*n*-Butane	4	10	0.970	−35.29
3	Isopentane	5	12	1.540	−42.95
4	*n*-Pentane	5	12	1.260	−41.40
5	2,2-Dimethylbutane	6	14	0.320	−51.00
6	2,3-Dimethylbutane	6	14	0.320	−49.48
7	2-Methylpentane	6	14	1.130	−48.82
8	3-Methylpentane	6	14	4.830	−48.28
9	Hexane	6	14	3.700	−47.52
10	Methylcyclopentane	6	12	0.820	−33.08
11	Cyclohexane	6	12	1.180	−37.34
12	2,2-Methylpentane	7	16	6.319	−57.05
13	2,3-Methylpentane	7	16	4.140	−55.81
14	3-Metylhexane	7	16	7.189	−54.35
15	Heptane	7	16	4.140	−53.63
16	Isooctane	8	18	0.270	−61.97
17	2,3 + 2,2-Dimethylhexane	8	18	1.590	−60.40
18	2,3,4-Trimethylpentane	8	18	0.270	−60.98
19	2,3,3-Trimethylpentane	8	18	0.270	−60.63
20	2-Methylheptane	8	18	22.258	−60.98
21	Octane	8	18	1.860	−59.74
22	Benzene	6	6	10.209	11.72
23	Toluene	7	8	14.429	2.87
24	*m*-Xylene	8	10	4.220	−6.07
25	*p*-Xylene	8	10	1.760	−5.84
26	*o*-Xylene	8	10	1.760	−5.84
27	Ethylbenzene	8	10	0.700	−2.98
28	*p* + *o* + *m*-Diethylbenzene	10	14	1.060	−17.44
29	1,2,4-Trimethylbenzene	9	12	1.060	−14.78

Table 2
Data of the fractional distillation of gasoline

Fuel characteristics	Base gasoline	Model gasoline
C/H ratio	0.539	0.539
Low heating value (MJ/kg)	44.5	43.1
Data of fractional distillation (°C):		
Start point	42	38
10 wt.%	73	71
50 wt.%	112	110
90 wt.%	165	170
End	185	182
Density (g/ml) (20 °C)	0.78	0.8

to-hydrogen ratio, low heating value, distillation curve (Table 2), and fractional composition (Fig. 4) to the real gasoline. The equilibrium model is based on the following simplifications: uniform temperature and pressure are assumed; no information about actual reaction pathways/formation of intermediates; no tar, no solid carbon are modeled; no information about the rate of the reactions. Besides the species listed in Table 1 were H_2, CO, CO_2, H_2O, CH_4, C_2H_2, C_2H_4, C_2H_6, C_3H_6, C_3H_8. Syngas formation by gasoline reforming with air and steam was investigated using calculations of thermodynamic equilibrium in the given chemical system as a function of oxygen-to-carbon ratio, steam-to-carbon ratio, temperature, pressure, and product species. The Peng–Robinson equations of state were used to calculate the stream properties. The HYSYS software package (HyproTech. HYSYS.Process.v2.2 AEA Technology) has been used for simulation purposes.

4. Results and discussion

The experimental data and the thermodynamic modelling ability to fit the data are presented in Table 3 and Fig. 5. For the thermodynamic calculations performed with the surrogate gasoline (Fig. 5), it was assumed that the reactor is adiabatic, which means that there is no heat transfer to or from the reactor, and that the reactant input parameters (the temperature and oxygen-to-carbon ratio) correspond to the experimentally measured values. The adiabatic temperature rise was calculated as a difference between the temperature of the feed and the back face temperature of the catalyst bed in the experimental reactor. A fair qualitative and quantitative agreement of calculated and measured values is observed for the concentration of components in the product gas, and adiabatic temperature rise, in particular, at the feed temperature of 190–210 °C.

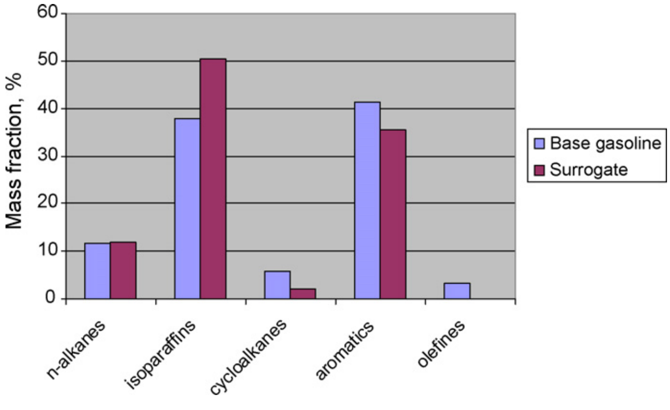

Fig. 4. Fractional composition of the base gasoline and its surrogate mixture.

In the paper the thermodynamic equilibrium restrictions on the syngas formation from gasoline were studied in comparison with isooctane and methane used for the same purpose to illustrate more clearly some peculiarities of the process. Effect of the preheat temperature on the temperature in adiabatic reactor and product gas is shown in Fig. 6. Contrary to the methane partial oxidation, where the input temperature can exert an important effect on the reaction temperature and syngas formation, the product composition at gasoline reforming is hardly affected by the preheat temperature of the feed. The predicted increase in the reaction temperature against the preheat temperature is not consistent with the experimental observations for the gasoline reforming. According to our measurements (see Fig. 7, left), the catalyst temperature was increased slightly with an increase in the temperature of gasoline–air mixture only up to about 240 °C and then decreased with further preheating. The reason is a higher reactivity of the gasoline fuel towards cracking compared to methane, especially in the mixture with air. The fractional composition of gasoline was observed to be altered at 200 °C preheats of the feed (Fig. 7, right). It was found that the preheat temperature of about 190 °C is a preferable one in the practical point of view.

It is desirable for reformed gas to contain a level of the H_2 concentration as high as possible. Obviously, the concentration of hydrogen in the product gas will depend on the number of hydrogen atoms per carbon in the fuel. According to the simple calculations of the reaction stoichiometry, the maximum achievable concentration of hydrogen for the fuels considered decreases in the order: methane (41%) > isooctane (28.1%) > gasoline (24.3%). However, reactivity of the specific fuel and their components also affect the actual product composition in the reforming process. The level of hydrogen in the product gas and whetherthe temperature in the monolith reactor at gasoline reforming were found to be much more affected by an air–fuel ratio in the feed than those for methane and even for isooctane (Fig. 8). For example, for methane partial oxidation, the low reaction heat evolved and weak dependence on the O_2/C ratio is observed, and to improve the actual conversion to synthesis gas, it is desirable not only to heat the feed mixture to the high preheat temperature, but also to operate at the O_2/C ratio of about 0.6 which is higher than stoichiometric one (see also Ref. [19]). Moreover, a region near the maximum of the hydrogen concentration is moderately flat, suggesting that a significant range of operating conditions could give good results. Optimal processing of gasoline, in terms of the adiabatic temperature and the hydrogen concentration, occurs in the restricted range of 0.50–0.52, when the concentrations of hydrogen in the product gas correspond to the calculated values of 24.08–23.15 mol%, respectively (dry level). At the fixed input temperature (200 °C) the adiabatic temperature rise increases from 787 at the molar ratio of 0.5 to 840 °C at $O_2/C = 0.52$. The higher O_2/C molar ratio may cause deactivation of the catalyst due to the high tem-

Table 3
Data on autothermal reforming gasoline to synthesis gas

Parameter	Run 1 ($O_2/C = 0.48$; $H_2O/C = 1.17$)			Run 2 ($O_2/C = 0.52$; $H_2O/C = 0.89$)			Run 3 ($O_2/C = 0.48$; $H_2O/C = 0.86$)		
	Experiment	Predicted data		Experiment	Predicted data		Experiment	Predicted data	
		Isothermal reactor at T_{out}	Adiabatic reactor at T_{in}		Isothermal reactor at T_{out}	Adiabatic reactor at T_{in}		Isothermal reactor at T_{out}	Adiabatic reactor at T_{in}
Gasoline (kg/h)	1.86			0.893			1.86		
Air (m^3/h) (STD)	6.90			3.58			6.98		
Water (kg/h)	3.13			1.14			2.3		
Q (m^3/h) (STD)	11.22			5.17			10.18		
Contact time (s) (at STD)	0.059			0.128			0.065		
Superficial velocity (m/s) (STD)	1.36			0.63			1.23		
Feed temperature, T_{in} (°C)	260			280			250		
Front (back)-face temperature, T_{out} (°C)	763 (860)			1050 (1000)			958 (898)		
Synthesis gas (dry) composition (mol%):									
H_2	31.7	31.8	32.0	27.5	27.9	28.1	30.3	30.4	30.6
CO	15.6	15.9	15.6	17.4	18.1	17.6	18.2	16.0	15.7
CO_2	9.6	8.4	8.6	7.1	6.4	6.6	6.3	6.5	6.8
N_2	45.1	43.4	43.3	49.4	47.3	47.0	46.3	44.3	44.2
CH_4	Trace	0.0036	0.0057	Trace	0.0002	0.0004	Trace	0.0025	0.0047
C_2–C_3	0			0			0		
Predicted adiabatic temperature (back face) (°C)			840			977			869

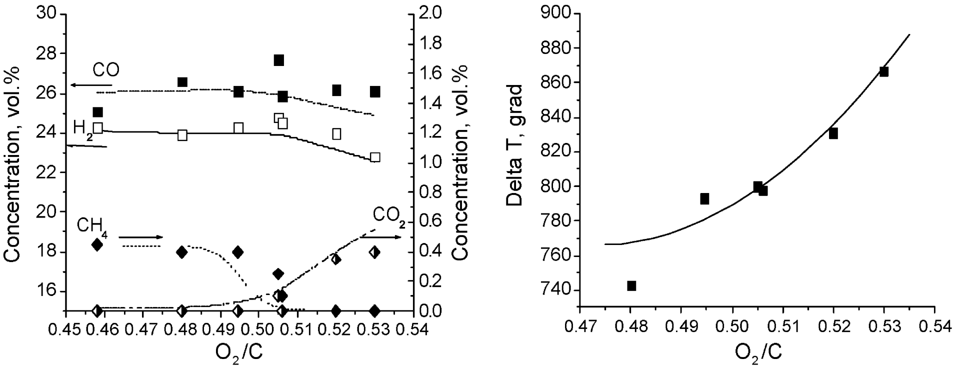

Fig. 5. Experimentally measured values (symbols) and thermodynamic predictions (curves) for the product gas (left) and adiabatic temperature rise (right) in the partial oxidation of gasoline vs. O_2/C molar ratio in the feed stream.

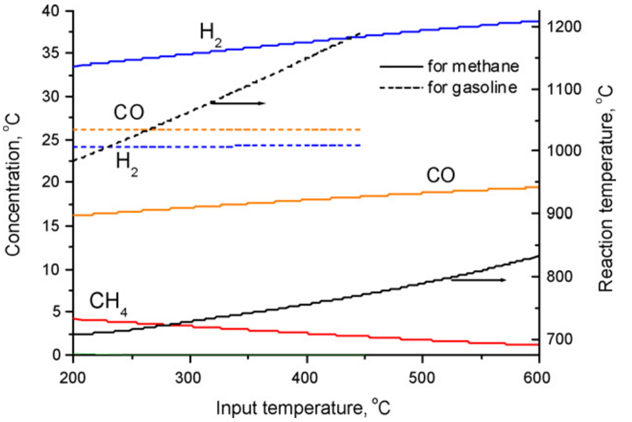

Fig. 6. Thermodynamic predictions on the effect of the feed temperature for the partial oxidation of methane and gasoline by air at adiabatic conditions. $O_2/C = 0.50$, $P = 1.0$ bar.

perature in the frontal part of the monolith, as it was observed in Ref. [15]. Compared to gasoline, moderate heat evolved and smaller increase in the temperature, about 40°, is observed for isooctane in the same range of the O_2/C ratio. This enables operating at the higher values of O_2/C ratios in the isooctane–air mixture.

The experimental data accompanied by thermodynamic calculations for the corresponding operational conditions of the reforming process when water vapor is added to the reaction mixture are presented in Table 3. The calculations of equilibria at the back face temperature (isothermal reactor) suggest that the product gas composition in the experiments is determined by the outlet temperature. It can be seen that using the surrogate gasoline, the predictions for the product distribution are in very good agreement with the measurements. Effects of the reaction temperature and such parameters of the feed gas as the steam and oxygen-to-carbon ratios are highlighted in Figs. 9 and 10. At the fixed values of the input temperature and O_2/C ratio in the feed, there is an equilibrium limit for the relative content of hydrogen in syngas. A well-defined maximum is observed in the hydrogen concentration plots for all the fuels considered in the thermodynamic calculations (Fig. 9, left). However, the temperature is to be high enough to minimize by-products formation also. At the temperature of 700 °C some amount of CH_4 may be formed even at the high value (0.52) of oxygen-to-carbon ratio in the gasoline autothermal reforming (Fig. 9, right). It is also important to feed sufficient oxygen so that the energy generated by the oxidation compensates the energy absorbed by the endothermic reactions. A high level of hydrogen is observed at the H_2O/C molar ratio of 1.0 in the range of the O_2/C ratio considered (Fig. 10, left). This value will correspond to the maximum reformer efficiency, because further increasing in the hydrogen yield would require an additional energy input to dry the reformate gas. Changing the H_2O/C ratio from 0.7 to 1.0 affects only slightly the amount of hydrogen formed for the given value of O_2/C, in contrast to the effect on the temperature in adiabatic reactor (Fig. 10, right). To keep the adiabatic temperature about 800 °C for the given input temperature of 270 °C and steam-to-carbon ratio of about 1.0, the oxygen-to-carbon ratio needs to be maintained at the value of about 0.45. At these operational parameters the thermodynamic

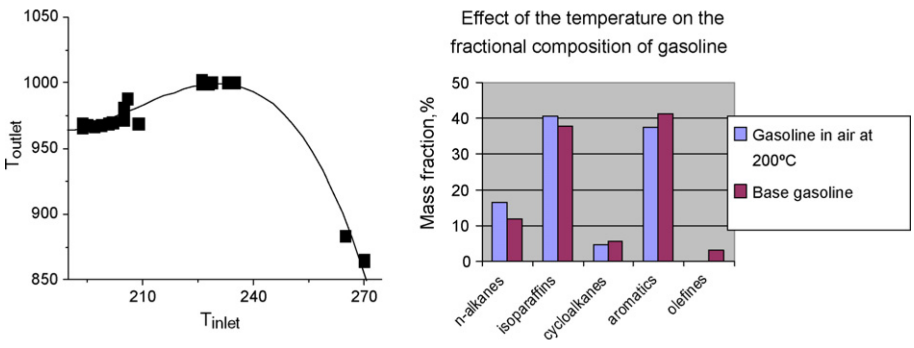

Fig. 7. Effect of the inlet temperature on the feed composition (right) and the outlet temperature (left).

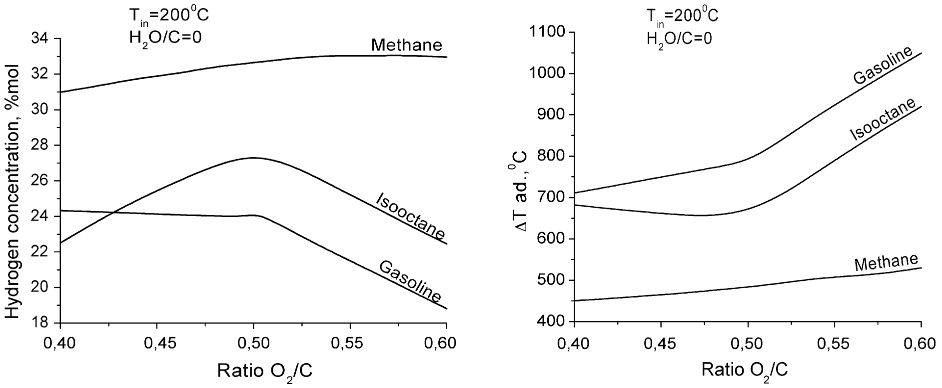

Fig. 8. Effect of the molar oxygen-to-carbon ratio in the fuel–air mixture on the hydrogen concentration and adiabatic temperature rise at the partial oxidation of methane, isooctane and gasoline with air.

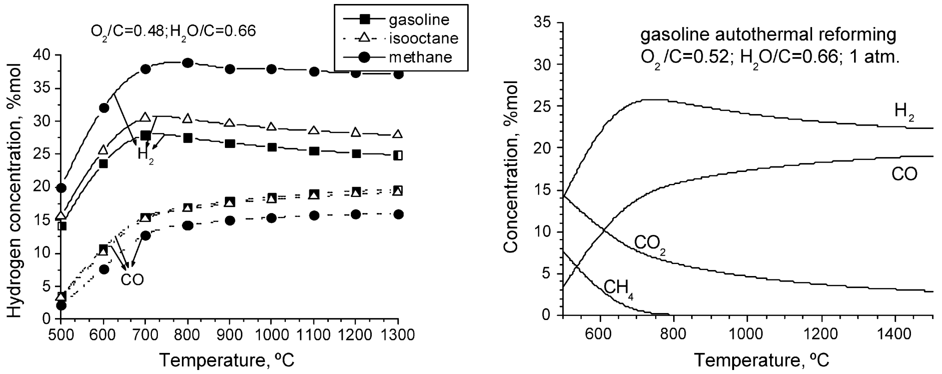

Fig. 9. Effect of the reactor temperature on equilibrium composition at autothermal reforming of the indicated fuels.

calculations predict the hydrogen concentration in the product gas of about 29 mol%.

In spite of the known fact that the hydrocarbons reforming reactions proceed quickly and equilibrates rapidly, both radial and axial temperature gradients are developed in a monolith reactor with the short contact time [15,19]. The readings of thermocouples centrally located along the reactor axis were used to illustrate the typical temperature profile in Fig. 3, and to be applied for the thermodynamic considerations in Fig. 5 and Table 3. The difference between the axial temperatures in the monoliths and at their periphery, near the reactor wall, did not exceed 30° in the frontal part and 70° at the outlet, in case of the partial oxidation reforming gasoline. Corresponding gradients observed in the autothermal reaction operation mode were about 20° and 40°, respectively. The metallic monolith catalysts employed in our experiments secured an extremely efficient dissipation of reaction heat through, a proper choice of support material and monolith geometry. Nevertheless, in the range of the experimental parameters applied, the longitudinal gradients of about 100° for the partial oxidation reforming and of 60–80° for the gasoline–air–steam (autothermal reforming) feed mixture were detected in the metallic monolith catalyst bed. At the high throughputs, the back face temperature may exceed the front face one (see run 1 in Table 3). The temperature profiles in the catalyst bed are results of interplay among kinetics, hydrodynamics, and heat transfer. The thermodynamic analysis allows

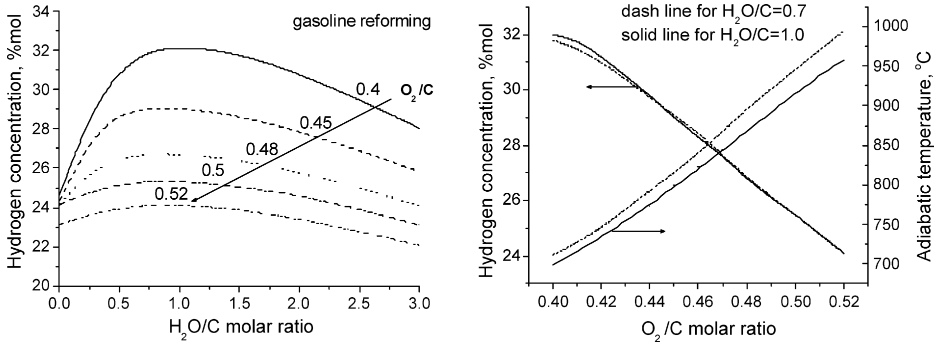

Fig. 10. Effect of the H_2/C and O_2/C molar ratio on the hydrogen concentration and adiabatic temperature in the gasoline autothermal reforming reactor. Feed temperature $T_{in} = 270\,°C$.

only outlining a range of the favorable operational conditions for the reforming system. For a practical consideration, the operational characteristics should be chosen on the basis of analysis of many factors including a range of throughputs, design of reactor and configuration of monoliths, as well as catalytic activity.

5. Conclusion

Both partial oxidation and autothermal reforming of gasoline containing 191 hydrocarbons were carried out at the metallic monolith with LaNiPt (1 wt.%)/LaRu (1 wt.%) active composition. It was found that doubling the flow rate at the constant oxygen-to-carbon ratio slightly affects the temperature distribution in the two monoliths loaded in the nearly adiabatic reactor. Longitudinal gradients of about 100° for the partial oxidation with air and of 60–80° for the gasoline–air–steam (autothermal reforming) feed mixture were detected in the catalyst bed. On the basis of the thermodynamic consideration with the surrogate mixture of 29 organics, it was found that optimal processing of gasoline by the partial oxidation with air occurs in the restricted range of 0.50–0.52, in which the concentration of hydrogen in the product gas corresponds to the theoretically predicted values of about 24 mol% (dry level). The product gas composition in the gasoline reforming is mainly determined by the catalyst outlet temperature. On addition of water in the feed, the optimal value for the H_2O/C molar ratio is found to be around 1.0 similar to isooctane and methane, while the oxygen-to-carbon ratio has to be adjusted to the temperatures of the feed and the actual catalyst employed. The thermodynamic predictions are in a good agreement with the experimental data obtained.

Acknowledgements

This work is in part supported by STC 2529 and RFBR 060381037 Projects. The authors highly appreciate an assistance of Gleb Urzhuntzev in this work.

References

[1] M.A. Rosen, D.S. Scott, Comparative efficiency assessments for a range of hydrogen production processes, Int. J. Hydrogen Energy 23 (8) (1998) 653–659F.

[2] F. Joensen, J.R. Rostrup-Nielsen, Conversion of hydrocarbons and alcohols for fuel cells, J. Power Sources 105 (2002) 195–201.

[3] T. D'Andrea, P.F. Henshaw, D.S-K. Ting, The addition of hydrogen to a gasoline-fuelled SI engine, Int. J. Hydrogen Energy 29 (2004) 1541–1552.

[4] M. Minutillo, On-board fuel processor modelling for hydrogen-enriched gasoline fuelled engine, Int. J. Hydrogen Energy 30 (13–14) (2005) 1483–1490.

[5] J.W. Zhu, G. Xiong, W. Han, W. Yang, Catalytic partial oxidation of gasoline to syngas in a dense membrane reactor, Catal. Today 93–95 (2004) 257–261.

[6] A. Docter, A. Lamm, Gasoline fuel cell systems, J. Power Sources 84 (1999) 194–200.

[7] S. Ahmed, M. Krumpelt, Hydrogen from hydrocarbon fuels for fuel cells, Int. J. Hydrogen Energy 26 (4) (2001) 291–301.

[8] A.E. Lutz, R.W. Bradshaw, L. Bromberg, A. Rabinovich, Thermodynamic analysis of hydrogen production by partial oxidation reforming, Int. J. Hydrogen Energy 29 (2004) 809–816.

[9] H.H. Ibrahim, R.O. Idem, Kinetic studies of the partial oxidation of isooctane for hydrogen production over a nickel–alumina catalyst, Chem. Eng. Sci. 61 (2006) 5912–5918.

[10] P. Dagaut, On the kinetics of hydrocarbons oxidation from natural gas to kerosene and diesel fuel, Phys. Chem. Chem. Phys. 4 (2002) 2079–2094.

[11] J.R. Rostrup-Nielsen, Singas in perspective, Catal. Today 71 (2002) 243–247.

[12] M. Pekar, What can kinetics learn from rational thermodynamics, Chem. Eng. Sci. 59 (2004) 4103–4112.

[13] V.N. Parmon, Chemical thermodynamics far from equilibrium: is it possible to develop it? Russ. J. Phys. Chem. 77 (2003) S128–S134.

[14] A.Q. Clark, S.E. McBsin, J. Kilner, Vapour–liquid equilibrium of (ethers + hydrocarbons or methanol or water) for motor gasoline modeling, Fluid Phase Equilib. 133 (1997) 239–246.

[15] L. Bobrova, I. Zolotarskii, V. Sadykov, S. Pavlova, O. Snegurenko, S. Tikhov, V. Korotkich, T. Kuznetsova, V. Sobyanin, V. Parmon, Syngas formation by selective catalytic oxidation of liquid hydrocarbons in a short contact time adiabatic reactor, Chem. Eng. J. 107 (2005) 171–179.

[16] L. Bobrova, I. Zolotarsky, V. Sadykov, V. Sobyanin, Hydrogen-rich gas production from gasoline in a short contact time catalytic reactor, Int. J. Hydrogen Energy (2006), in press.

[17] S.N. Pavlova, et al., Patent RU No. 2,248,932, 2003.

[18] V.A. Sadykov, S.N. Pavlova, R.V. Bunina, G.M. Alikina, S.F. Tikhov, T.G. Kuznetsova, Yu.V. Frolova, A.I. Lukashevich, O.I. Snegurenko, N.N. Sazonova, E.V. Kazantseva, Yu.N. Dyatlova, V.V. Usol'tsev, I.A. Zolotarskii, L.N. Bobrova, V.A. Kuz'min, L.L. Gogin, Z.Yu. Vostrikov, Yu.V. Potapova, V.S. Muzykantov, E.A. Paukshtis, E.B. Burgina, V.A. Rogov, V.A. Sobyanin, V.N. Parmon, Selective oxidation of hydrocarbons into synthesis gas at short contact times: design of monolith catalysts and main process parameters, Kinet. Catal. 46 (2005) 227–250.

[19] Y.-S. Seo, A. Shiley, S.T. Kolaczkowski, Evaluation of thermodynamically favourable operating conditions for production of hydrogen in three different reforming technologies, J. Power Sources 108 (2002) 213–225.